Robotic Force Estimation using Dithering to Decrease the Low Velocity Friction Uncertainties

Andreas Stolt, Anders Robertsson, Rolf Johansson

Abstract— **For using industrial robots in applications where the robot physically interacts with the environment, such as assembly, force control is usually needed. A force sensor may, however, be expensive and add mass to the system. An alternative is therefore to estimate the external force using the motor torques. This paper considers the problem of force estimation for the case when the robot is not moving, where the Coulomb friction constitutes a fundamental difficulty. A dithering feedforward torque is used to decrease the Coulomb friction uncertainty, and hence improve the force estimation accuracy when the robot is not moving. The method is validated experimentally through an implementation on an industrial robot. A lead-through scenario is also presented.**

I. INTRODUCTION

Industrial robots have traditionally been position controlled, i.e., controlled to follow predefined trajectories. They are very good at trajectory following, being both very accurate and working at high speeds, and they have become indispensable in many places doing tasks such as welding, painting, and pick-and-place operations. Other types of tasks, which require interaction with the environment, such as assembly and machining, have been less robotized. Uncertainties in the tasks make it hard to use a position-controlled robot to solve them, as the accuracy required, of the work-cell and the robot, becomes very high. A solution is to introduce external sensing, such as a force sensor or a vision system. A force sensor can for instance give the robot capability to correct for small position uncertainties by sensing the contact forces.

A force sensor may also be used for easy programming of a robot. By letting the robot be manually guided by an operator, a lead-through scenario, the robot can easily be taught what to do. A force sensor may, however, be too expensive, especially if lead-through is the only intended use. A sensor may also be sensitive to different environments, e.g., varying temperatures, and it may add unnecessary mass to the system, i.e., reducing the effective workload. An alternative is therefore to estimate the external forces, by using sensing already available in the robot. This usually means the position sensors in the joints and the motor torques. Previous work using the position sensors have usually been model-based disturbance observers, e.g., [1], [5]. Examples of works based on motor torques are [10], [12].

When a robot is not moving, the main disturbance for force estimation is the Coulomb friction. It is usually quite

Andreas Stolt, `andreas.stolt@control.lth.se`, Anders Robertsson, and Rolf Johansson are with the Department of Automatic Control, LTH, Lund University, Sweden.

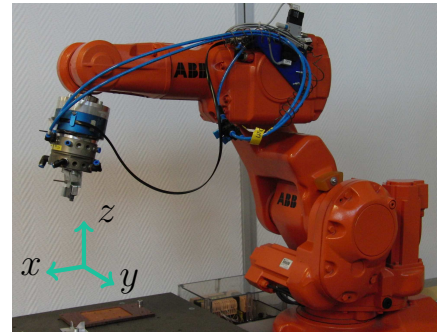The authors are members of the LCCC Linnaeus Center and the eLLIIT Excellence Center at Lund University.

Fig. 1. The ABB IRB140 robot used in the experiments. The wrist-mounted JR3 force/torque sensor (blue cylinder) was used for verification of the estimated entities. The reference coordinate frame is also displayed.

large for industrial robots, which often have gear boxes with high gear ratios. This means that large external forces are needed to overcome the friction and make it possible to estimate the force. When the robot is not moving, the friction force may be anywhere within the friction band, and the force to overcome the friction is thus unknown. Previous research has been performed about compensating for friction, e.g., in [6] the dynamic LuGre model was used for friction compensation. For force estimation, however, knowing the friction more in detail will not give better estimates, as the external force still must overcome it. By using a feedforward torque within the friction band, however, the torque can be controlled to be close to the border of the friction band. Then, only a small force is needed to overcome the friction. This feedforward torque may be in the form of a dithering signal, i.e., a high-frequency zero-mean signal.

Dithering has previously been used, for instance, to suppress quantization effects. This has been done by adding the dithering signal as a noise signal. A survey of its use in audio signal processing is presented in [11]. Another application where dithering was used to suppress quantization effects is precise current control [13]. Dithering has also been used in the context of robotics. In [8], [9] dithering was used in assembly tasks to overcome friction between the parts, which corrupted the force measurements. It was further presented how the dither parameters could be tuned online. Dithering can also be used to compensate for stiction in valves. In [7] a dithering-like signal was added to the control signal to compensate for stiction in pneumatic control valves in the process industry.

This paper considers the problem of force estimation when the robot is not moving and subject to Coulomb friction.

A dithering signal was used to decrease the static friction uncertainty, and hence increase the force estimation accuracy. The method was implemented and tested experimentally with an industrial robot in a lead-through scenario. The experimental setup is displayed in Fig. 1, where the fixed work-space reference directions are illustrated.

A similar approach where force estimation was performed together with dithering to suppress the friction uncertainties is presented in [4]. The external torque applied to each joint of the robot was estimated through disturbance observers, and a dithering signal was used to make the robot more sensitive to external forces. The paper presents multiple interesting results, but without enough details to make them reproducible or to make relevant comparisons.

II. FORCE ESTIMATION

The method for force estimation used in this paper is presented in [10] — a summary of the method is given here. The force estimation is based on the measured motor torques, τ_m, which are modeled to consist of

$$\tau_m = \tau_{grav} + \tau_{dynamic} + \tau_{ext} + \tau_e \qquad (1)$$

The gravity torques, τ_{grav}, are assumed to be known and can be compensated for. The dynamic torques, $\tau_{dynamic}$, are neglected, as slow velocities and low accelerations are expected in the types of tasks where force estimation is used. The external torques, τ_{ext}, are assumed to originate from forces applied to the end effector of the robot, and thus given by

$$\tau_{ext} = J^T F \qquad (2)$$

where $J = J(q)$ is the robot Jacobian, q the joint coordinates, and F the force/torque applied to the end effector.

The disturbance torque, τ_e in (1), is modeled to consist of friction and measurement noise, $\tau_e = \tau_f + e$. The friction torques, τ_f, are velocity dependent, and mainly consist of Coulomb and viscous friction. The Coulomb friction can be modeled as a constant torque for large velocities, but for low or zero velocities it can end up in quite a large interval. Therefore, it is modeled to be the outcome of a uniformly distributed random variable with a velocity dependent range. The noise, e, is assumed to be Gaussian with zero mean and covariance R_e. The total disturbances, τ_e, are thus modeled to be the sum of a uniformly distributed and a Gaussian random variable.

Assuming that the prior on F is Gaussian with $\mathbb{E}[F] = \bar{F}$ and $\mathbb{E}[(F - \bar{F})(F - \bar{F})^T] = R_F$, and that F and τ_e are uncorrelated, the Maximum Likelihood (ML) estimate of F is given by the F solving

$$\begin{aligned} \underset{\text{over } F, \tau_f}{\text{minimize}} \quad & \left(\bar{\tau} - J^T F - \tau_f\right)^T R_e^{-1} \left(\bar{\tau} - J^T F - \tau_f\right) \\ & + \left(F - \bar{F}\right)^T R_F^{-1} \left(F - \bar{F}\right) \\ \text{subject to} \quad & \tau_{f,min} \leq \tau_f \leq \tau_{f,max} \end{aligned}$$
$$\qquad (3)$$

where $\bar{\tau} = \tau_m - \tau_{grav}$ is the motor torques compensated for gravity torques. The range of the uniform part of the disturbance torques are described by the inequality constraint. The
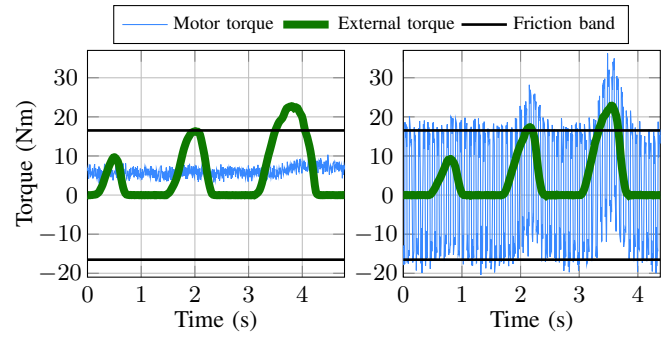

Fig. 2. Resulting torques for one joint from an experiment where forces were manually applied to the robot, without dithering in the left diagram and with dithering in the right diagram.

optimization problem (3) is convex and of low order, and it can therefore be solved reliably in real time.

The uncertainty in the force estimate varies significantly depending both on the motion of the joints and the configuration of the robot through the Jacobian. A confidence interval estimate can therefore also be calculated, see [10] for how this can be performed. Further, note that the optimization problem (3) can be solved also when the Jacobian, J, is singular. The force estimate will then rely on the prior, but the confidence interval will be huge in the singular direction, i.e., reflecting the uncertainty of the estimate.

III. DITHERING

A. One joint

To see the benefit for force estimation of using dithering, a simple experiment was first performed. A force was applied to the robot by manually pushing its end effector, and the resulting motor torque for one of the joints is shown in the left diagram in Fig. 2. The diagram also contains the external torque, τ_{ext}, as measured by a force sensor, and an estimate of the Coulomb friction band. It can be seen that there is not much of a response in the motor torque data, although the last push exceeded the friction band. The joint controller was active in the experiment, controlling the position of the joint, otherwise the last push would have resulted in the robot starting to move.

The same experiment as above was conducted once more, but this time with a torque feedforward dithering signal, see the right diagram in Fig. 2. The last two pushes are now clearly visible in the motor torque data, and almost the first one as well. By adding the dithering signal, it is thus possible to detect smaller forces than was possible without the dithering. This result is similar also for the other joints of the robot.

B. Dithering signal generation

The dithering signal used in this paper was a square wave, and it was sent to the robot system as a torque feedforward signal, τ_{ffw} in the block diagram of the joint controller in Fig. 3. When the robot is not moving, the torque for each joint may be anywhere within the Coulomb friction band.
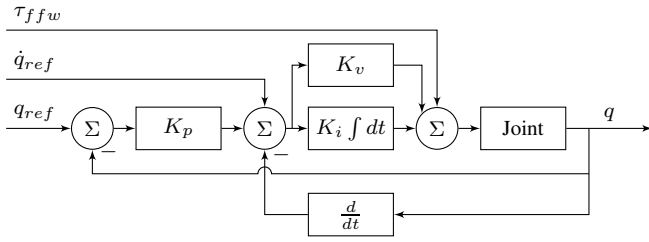
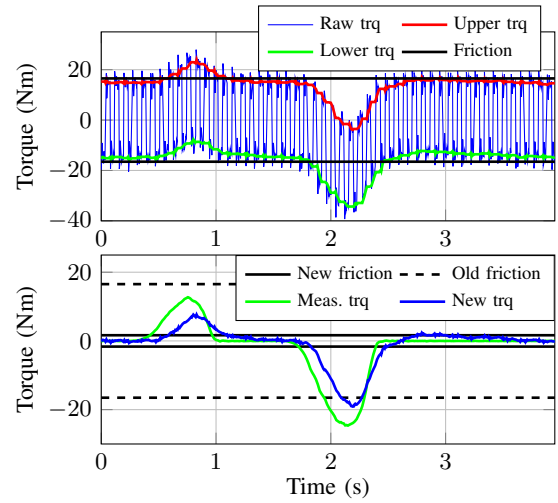Fig. 3.   Schematic robot joint control block diagram.

Fig. 4.   Illustration of how the torque signal and Coulomb friction bounds are extracted. The upper diagram displays how an upper and a lower torque signal are calculated. The lower diagram shows the new torque signal, the mean of the upper and lower torque in the upper diagram, together with the external torque, as measured with a force sensor. The new and old friction band estimates are also displayed.

Therefore, to center the dithering signal inside the friction band requires some control. A feedback control scheme was used in this case. To be able to control the center at all, the position loop in the joint controller had to be disabled, i.e., setting $K_p = 0$ in Fig. 3. Otherwise, the position control loop would counteract any static torque feedforward. One reason for this could be that the motor could move slightly without moving the arm side of the joint, with the gears acting as a spring for torques within the friction band. The reference for the center torque was in the middle of the estimated friction band, i.e., the estimated torque due to gravity. The center of the measured torque signal was calculated as the mean over an integer number of periods of the dithering signal. An integral controller was used for closing the feedback loop.

The amplitude of the dithering signal also had to be controlled. The motor torque measurements were actually the reference sent to the current control loop in the motor, as true motor torque could not be measured. This means that to be able to detect external torques, the joint controllers had to be active. However, this also resulted in the control counteracting the dithering signal, meaning that a slightly larger feedforward signal was needed than the desired torque response. A feedback loop with an integral controller solved this problem. The amplitude was calculated as the mean of half the difference of all samples above and below the center for an integer number of periods of the dithering signal. The pseudo-code below was used for the calculation:

function CALCDITHERSIGNALPARS(trq)
    trqHistory ← [trq , trqHistory(1..end-1)]
    center ← mean(trqHistory)
    upLevel ← mean(trqHistory>center)
    lowLevel ← mean(trqHistory<center)
    amplitude ← (upLevel-lowLevel)/2
    return center, amplitude
end function

The variable trqHistory is a persistent variable between calls to the function, and it contains a history of the torque for an integer number of dithering periods. The calculation of upLevel (and lowLevel) is done by taking the mean of all samples being greater than (lower than) the mean of trqHistory.

When an external torque appears, the feedback controllers will try to counteract the deviations. But as the measurement signals are based on an average over the last periods, and as the control loops are not too tight, it will be possible to detect

the external torque. Once it has been detected, the robot is supposed to act upon it and turn off the dithering signal.

The set-point amplitude for each joint was chosen as large as possible before the dithering signal resulted in a vibrating robot. About one hundredth of a motor radian, which would correspond to 0.0001 arm radians, was chosen as an acceptable level of vibration. The dithering amplitude for the different joints varied between 50-90 % of the estimated friction band.

IV. FORCE ESTIMATION USING DITHERING

A. Extracting torque signal and friction bounds

As was seen in Fig. 2, when a joint was fed with a dithering signal, the external torque appeared as a superimposed signal on the dithering signal. Actually, the external torque appeared on both sides of the dithering signal. Another example of a dithered joint where an external torque has been applied is displayed in the upper diagram of Fig. 4. The two curves marked as upper (red) and lower torque (green) are the one-period means of all samples above and below the mean of all samples within the last dithering period, respectively. The mean of these two signals should be an estimate of the applied external torque. Taking the mean has the effect that it shifts the signal to the center of the dithering signal, as well as taking away some noise. The lower diagram of Fig. 4 shows the estimate together with the actual external torque, as measured by a force sensor for verification. Whereas the actual torque is underestimated, the shape of the signal is captured. A slight response delay can also be seen.

As the external torque signal is added to the dithered signal, only a small external torque is required to exceed the friction band. This has the effect that the friction band is effectively decreased. In Fig. 4 the set-point for the dithering signal was 90 % of the friction band, and thus only 10 %

of the friction band remained. This is illustrated in the lower diagram in Fig. 4, where the new friction band is the old friction band shifted down with the dithering set-point amplitude.

B. Dithering on several joints

When dithering signals are sent to all joints of the robot simultaneously, there might be interactions between the joints which amplifies the vibration. This meant that the dithering amplitude had to be decreased for some of the joints, compared to when the joints were dithered separately.

V. APPLICATION SCENARIO

The dithering method was implemented in a lead-through scenario, i.e., to let the user guide the robot by holding on to the end effector (or to any other part of the robot). For the force estimation, it was assumed that all external forces were applied at the end effector. This means that the torques around the end effector will be small, and this information was used for choosing the prior, $\bar{F} = 0_{6 \times 1}$ and $R_f = \mathrm{diag}(20\,(\mathrm{N}), 20\,(\mathrm{N}), 20\,(\mathrm{N}), 0.3\,(\mathrm{Nm}), 0.3\,(\mathrm{Nm}), 0.3\,(\mathrm{Nm}))^2$ in (3), i.e., forces of $20\,\mathrm{N}$ expected and only small contact torques. Dithering was initiated when the robot was still, and it was turned off when a force was detected that made the robot move.

Only linear movements were allowed, due to the difficulty of estimating external contact torques. Long lever arms make estimation of forces beneficial, while the low signal-to-noise ratio for torques makes it almost impossible to estimate them, at least when only small contact torques are expected, as in the lead-through scenario.

The lead-through was accomplished by using a force controller, which was implemented as an impedance controller in task space with zero stiffness. To avoid that noise and incorrect force estimates moved the robot, a deadzone of $10\,\mathrm{N}$ was used on the force estimate. Another option could have been to use the confidence interval estimate and avoid using a deadzone, by setting the force to zero if the interval contains zero, and otherwise use the limit with the lowest magnitude. The confidence interval width, however, decreases rapidly when the robot starts to move, which results in that the force driving the robot will either be zero or quite large. The resulting robot motion would then be quite jerky and thus be discomforting for the operator.

VI. EXPERIMENTAL RESULTS

A. Robot system

The robot system used in the experiments in this paper was an ABB IRB140. It was controlled with the ABB IRC5 control system. As illustrated in Fig. 3, each joint of the robot was individually controlled with a cascaded structure. Position and velocity references, and torque feedforward, were sent from the trajectory generator in the main computer of the control system. The IRC5 system was extended with an open control system [2], [3], which made it possible to modify the reference signals and read measurements from the robot. Actually, the motor torque measurement was the
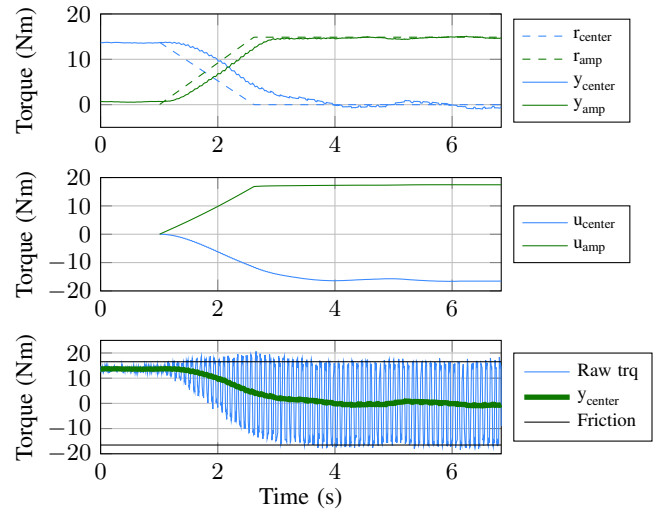

Fig. 5. An example of the dithering signal control performance. The top diagram shows the reference and the measurement signals. The middle diagram displays the control signals. No reference or control signal are displayed until dithering is activated, which happens at $t = 1\,\mathrm{s}$. The bottom diagram shows the actual motor torque signal together with the center torque measurement and the friction band estimate.

reference sent to the current controller in the motor, closely approximating the actual motor torque due to tight control and the fact that the current loop ran with a frequency of $2\,\mathrm{kHz}$ while the torque measurement was sampled at $250\,\mathrm{Hz}$. A wrist-mounted JR3 force/torque sensor was used for verification of the estimated forces. The external joint torques were calculated as $\tau_{ext} = J^T F_{sens}$, where J is the robot Jacobian and F_{sens} the force/torque measurement from the sensor.

The friction model parameters in (3), R_e, $\tau_{f,min}$, and $\tau_{f,max}$, were estimated from the same types of experiments as were used in [10]. The noise terms acting on the different joints were assumed to independent, such that R_e became diagonal.

B. Control of dithering signal

Experimental data from one joint showing the control of the dithering signal are given in Fig. 5. The top diagram shows the reference signals and the corresponding measurement signals for the center level and the amplitude of the resulting motor torque signal. They were calculated by averaging over the five last periods of the dithering signal. The dithering was started at $t = 1\,\mathrm{s}$, and it was ramped up to the final set-point, both the center and the amplitude, to get a smooth transition. The ramping is further important, as the torque before the dithering is started may be close to the friction band, as in Fig. 5, and starting the dithering signal with the full amplitude, there would be a large risk of getting a torque outside of the friction band such that the robot would start to move. The middle diagram displays the control signals, i.e., the static torque feedforward and the square wave amplitude. The bottom diagram shows the motor torque and the friction band estimate, and the center
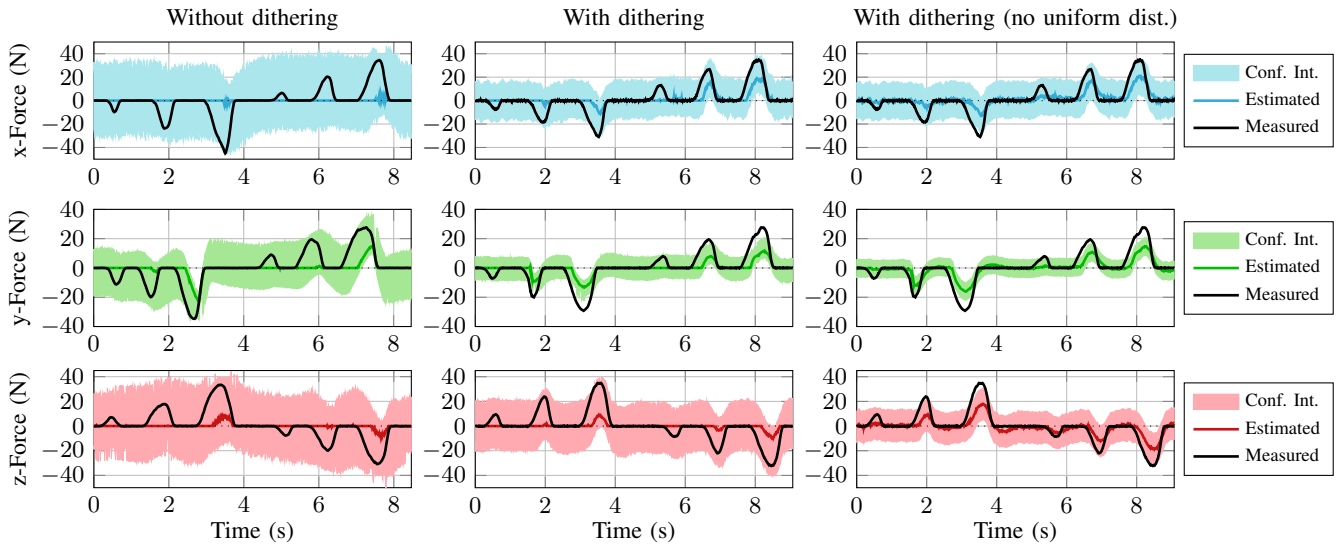
3899

Fig. 6. Estimated and measured forces from an experiment where external forces were applied to the end effector of the robot. The left column displays the result when no dithering was used, the middle column when dithering was used, and in the right column the dithering method was used without the Coulomb friction modeled as a uniformly distributed random variable.

measurement signal is also displayed. The angular frequency of the dithering signal was chosen to be $80\,\mathrm{rad/s}$.

The robot program was running with a sampling frequency of $250\,\mathrm{Hz}$, but the dithering control loops were only updated every 10th sample, i.e., running at $25\,\mathrm{Hz}$. The control signals were further kept constant when the measurement signals were close to the references, which here meant about $2\,\%$ of the estimated friction band. This means that the dithering signal can be seen as mostly a feedforward signal, and there will be time to detect applied external torques before the dithering control loops will start to eliminate the "disturbance", which the external torque will be interpreted as by the dithering control loops.

C. Comparison of using and not using dithering

Several experiments where external forces were applied to the robot in certain Cartesian directions were performed to investigate which magnitude of forces that could be detected. Forces were applied in each direction approximately 50 times. The robot was positioned such that each applied force would result in torques influencing at least one joint, see Fig. 1, which also shows the coordinate frame the forces are measured in. These experiments were first performed without using the dithering technique, i.e., using the force estimation method presented in [10], and some of the results are displayed in the left column in Fig. 6. Note that each subplot shows a separate experiment. In the middle column in Fig. 6, a corresponding result from when dithering was used is displayed. All confidence interval estimates were calculated according to the method presented in [10].

It can first be noted that when dithering was used, the force estimator was able to detect smaller forces in all directions. For the z-direction, however, the performance using dithering is only slightly improved as compared to without dithering. The second thing to notice is that the confidence interval

estimate is tighter for the dithering case, and even a little bit too tight for the y-direction. Also the forces can in general be seen to be underestimated. The explanation to this is partly that the prior used for force estimation drives the estimate towards zero when the optimization problem (3) is solved; the measurement is explained as friction instead of external force. When dithering is used, part of the explanation also lies in the tendency of the method to underestimate the applied torque, as was displayed in Fig. 4. The underestimation effect gets reduced when the external forces become larger, in relation to the friction torques, i.e., resulting in a decreased estimation error.

The confidence interval estimate seems to be overly pessimistic for both cases, especially when the external force was zero. But when external forces were present, it can be seen that the confidence interval seem to be more appropriate.

The confidence intervals sometimes seem to contain some information about the external force that is not visible in the actual force estimate, e.g., in the z-direction for the dithering case at $t = 2\,\mathrm{s}$, $t = 6\,\mathrm{s}$, and $t = 7\,\mathrm{s}$. The reason for this not showing up in the force estimate is that it is absorbed by the remaining Coulomb friction, when solving the optimization problem (3). The Coulomb friction is modeled by a uniformly distributed random variable, as it may be anywhere within in the friction band. For the dithering case, however, the torque is controlled to stay in the center of the friction band. The uniformly distributed part of the disturbance torques can therefore be ignored in the optimization problem. Doing this removes uncertainty from the problem, and this can be compensated for by increasing the variance of the noise parameter, which is modeled as a Gaussian random variable. The result of doing this is displayed in the right column in Fig. 6. The estimation performance in the x- and y-directions are similar, but the
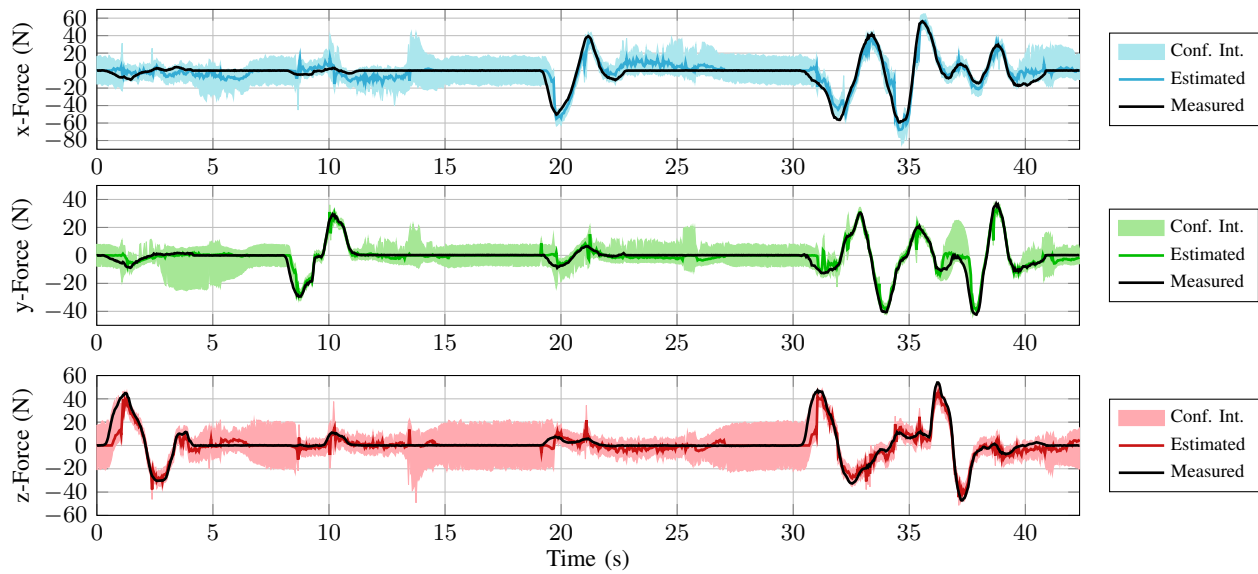
3900

Fig. 7.   Estimated and measured forces (for verification) from a lead-through experiment.

z-force estimate has improved significantly and it is now as good as in the other directions. An effect of ignoring the uniform term was that non-zero force estimates when the external force was zero were much more frequent, e.g., the x-force at $t = 6\,\mathrm{s}$ and the z-force at $t = 4\,\mathrm{s}$.

Based on all performed experiments, 50 in each direction, both without and with dithering, it was investigated how large the applied force had to be to give a response that exceeded the noise level in the estimated force. Without dithering, no force smaller than $32\,\mathrm{N}$ gave any response in the x-direction and $22\,\mathrm{N}$ in the y- and z-directions. With dithering, responses could be seen in all directions already for forces with a magnitude of $10\,\mathrm{N}$. It was also investigated how much force that was needed to estimate a force significantly different from zero, which here was chosen to be an estimated force above $10\,\mathrm{N}$. Without dithering an applied force of $40\,\mathrm{N}$ was needed in the x-direction and $30\,\mathrm{N}$ in the y- and z-directions. When dithering was used, an applied force of $20\,\mathrm{N}$ was enough in all directions.

D. Lead-through

A lead-through program was implemented that was using the estimated external force. Dithering was initiated when the robot was not moving, and turned off as soon as a force was detected that resulted in that the robot started to move. The transitions between dithering and not dithering were made smooth by ramping the dithering signal up and down, as was displayed in Fig. 5.

Experimental data from a lead-through experiment are displayed in Fig. 7. The robot was first moved in the z-direction, then in the y-direction, and then in the x-direction before the experiment was ended with the robot being moved in several directions simultaneously. It can be seen that the estimated force in general follows the measured force. During transfer from a zero-valued force to a non-zero value,

it can be seen that the estimate is lagging behind somewhat, e.g., the z-force at $t = 1\,\mathrm{s}$ and the x-force at $t = 20\,\mathrm{s}$. This is an effect that can be seen in other experiments as well, for instance, in Fig. 4.

The confidence interval estimate becomes significantly tighter when the robot starts to move, see for instance between $t = 30\,\mathrm{s}$ and $t = 40\,\mathrm{s}$, where the width of the interval is approximately halved, compared to when the robot is not moving. The reason for the increased confidence is that the Coulomb friction is now assumed to be known, and only uncertainty in the Gaussian noise parameter remains. There are some false force estimates, e.g., the x-force estimate around $t = 12\,\mathrm{s}$ and $t = 24\,\mathrm{s}$. The confidence interval still contains the measured force, though.

VII. DISCUSSION

When using the dithering method, there is a risk that a too high amplitude of the torque feedforward signal is used. Doing that would result in a vibrating robot, which would result in anything but a user-friendly experience. The amplitudes chosen in this paper were based on the measured motor angles, but also on the actual hands-on impression one got from the robot. Applying the dithering signal can be heard as a slight change in the sound coming from the motors, and it can be felt as a faint vibration when holding on to the end effector. It is, however, not discomforting. A person not aware of what is going on would probably not notice that much of difference from a robot not being applied to dithering. There is further a risk that the dithering signal will introduce unneccesary wear of the motors and the gear boxes. With the amplitude kept low and only used when needed, e.g., during lead-through, it should not be a problem.

The configuration of the robot is of high importance for the force estimation performance. If many joints can be used to estimate the force in a certain direction, then good estimates

and tight confidence intervals can be expected, as information from many joints are combined. For the experiments in this paper, the y-direction was a beneficial direction, while the other two, x and z, were slightly less beneficial. This could for instance be seen on the confidence interval estimates. When developing robot programs utilizing force estimation, the configuration of the robot is something the programmer has to bear in mind.

The dithering signal used in this paper was a square wave. Other types of wave forms are also possible and it remains as future work to try them out. The frequency of the dithering signal is also something that should be further investigated. The frequency used was the same for all experiments, and chosen to provide a satisfactory torque response. When using a high-frequency signal there is a risk that aliasing becomes a problem, but no such problem has been observed.

The experiments performed in this paper have shown that the torques due to external forces get underestimated. The reason for this could be that it is the motor torque reference that is the measurement, instead of the actual motor torque. For the reference to change, there have to be a position or velocity error, which may lead to a lower torque reference than the torque that was actually applied.

The applicability of force estimation depends on the task you intend to perform. Friction constitutes a fundamental difficulty that will give rise to estimation errors, which will limit the accuracy of force estimation. For the robot used in this paper, an external force of around $10\,\mathrm{N}$ was needed for the estimator to notice it and around $20\,\mathrm{N}$ for it to be certain that there actually was a force when the robot was not moving. This is a significant improvement compared to when no dithering was used, as forces with the magnitude of $20\text{-}30\,\mathrm{N}$ then were needed to get a reaction in the estimated force, and $30\text{-}40\,\mathrm{N}$ for the estimator to be certain that there actually was an external force present. Using dithering effectively decreases the Coulomb friction level, and increases the backdriveability of the robot. For the case when the robot is moving, the accuracy improves significantly, as the uncertainty in friction is much lower. For another robot with more or less friction, the accuracy will be different.

Other methods for force estimation commonly rely upon that a dynamical model of the robot is known, e.g., [1], [5], [12]. We do not have such a dynamical model available, and these methods have therefore not been tested.

Using the dithering method is only applicable in cases where the robot is not moving. The lead-through scenario investigated in this paper is one such example. Another possible application is dual-arm operations where one of the arms only supports the second arm, e.g., a screwing task where one of the arms performs the screwing operation while the other only holds the pieces being screwed together.

The use of dithering was shown to increase the accuracy of force estimation in the case when the robot was not moving. The performance is, however, still quite far from that of a force sensor. In the lead-through scenario, the improved accuracy is hard to notice, as quite large forces usually are applied, so large that they would be detected without dithering as well. But for another scenario where it would be important to detect forces of small magnitude, much could be gained by using dithering.

VIII. CONCLUSIONS

A method for improving the accuracy of force estimation when the robot is not moving was presented. It was based on using dithering as a feedforward torque signal. This made it possible to decrease the Coulomb friction uncertainty. Experimental results with an industrial robot verified that the method works, making it possible to detect forces of magnitudes around $10\,\mathrm{N}$, as compared to $20\text{-}30\,\mathrm{N}$ when no dithering was used. An implementation in a lead-through scenario was also presented.

ACKNOWLEDGMENT

REFERENCES

[1] A. Alcocer, A. Robertsson, A. Valera, and R. Johansson. Force estimation and control in robot manipulators. In *Proc. 7th IFAC Symp. Robot control (SYROCO)*, pages 31–36. Wrocław, Poland, Sep. 2003.

[2] A. Blomdell, G. Bolmsjö, T. Brogårdh, P. Cederberg, M. Isaksson, R. Johansson, M. Haage, K. Nilsson, M. Olsson, T. Olsson, A. Robertsson, and J. Wang. Extending an industrial robot controller–Implementation and applications of a fast open sensor interface. *IEEE Robotics & Automation Magazine*, 12(3):85–94, 2005.

[3] A. Blomdell, I. Dressler, K. Nilsson, and A. Robertsson. Flexible application development and high-performance motion control based on external sensing and reconfiguration of ABB industrial robot controllers. In *Proc. ICRA 2010 Workshop on Innovative Robot Control Architectures for Demanding (Research) Applications*, pages 62–66, Anchorage, Alaska, USA, May 2010.

[4] H. Cho, M. Kim, H. Lim, and D. Kim. Cartesian sensor-less force control for industrial robots. In *Proc. Int. Conf. Intelligent Robots and Systems (IROS)*, pages 4497–4502. Chicago, USA, Sep. 2014.

[5] K.S. Eom, I.H. Suh, W.K. Chung, and S.R. Oh. Disturbance observer based force control of robot manipulator without force sensor. In *Proc. Int. Conf. Robotics and Automation (ICRA)*, pages 3012–3017, Leuven, Belgium, May 1998.

[6] L. Freidovich, A. Shiriaev, A. Robertsson, and R. Johansson. LuGre-model-based friction compensation. *IEEE Transactions on Control Systems Technology*, 18(1):194–200, 2010.

[7] T. Hägglund. A friction compensator for pneumatic control valves. *Journal of Process Control*, 12(8):897–904, 2002.

[8] S.L. Ipri and H. Asada. Tuned dither for friction suppression during force-guided robotic assembly. In *Proc. Conf. Intelligent Robots and Systems (IROS)*, pages 310–315, Pittsburgh, USA, Aug. 1995.

[9] S. Lee and H. Asada. Direct adaptive control of force-guided assembly robots using tuned dither. In *Proc. American Control Conf. (ACC)*, pages 370–374, Seattle, USA, Jun. 1995.

[10] M. Linderoth, A. Stolt, A. Robertsson, and R. Johansson. Robotic force estimation using motor torques and modeling of low velocity friction disturbances. In *Proc. Int. Conf. Intelligent Robots and Systems (IROS)*, pages 3550–3556. Tokyo, Japan, Nov. 2013.

[11] S.P. Lipshitz, R.A. Wannamaker, and J. Vanderkooy. Quantization and dither: A theoretical survey. *Journal of the Audio Engineering Society*, 40(5):355–375, 1992.

[12] M. Van Damme, B. Beyl, V. Vanderborght, V. Grosu, R. Van Ham, I. Vanderniepen, A. Matthys, and D. Lefeber. Estimating robot end-effector force from noisy actuator torque measurements. In *Proc. Int. Conf. Robotics and Automation (ICRA)*, pages 1108–1113, Shanghai, China, May 2011.

[13] H. Zhu and H. Fujimoto. Overcoming current quantization effects for precise current control using dithering techniques. *IEEJ Journal of Industry Applications*, 2(1):14–21, 2013.